Influence of the natural wind speed on the performance of solar thermal façades

Edward Frick[1], Maik Kirchner[1] and Federico Giovannetti[1]

[1] Institute for Solar Energy Research in Hamelin (ISFH), Emmerthal (Germany)

Abstract

The solar thermal activation of the building envelope offers untapped potential for novel solutions based on renewable energy in multi-story buildings. Activated façades designed as uncovered collectors are particularly suitable for the support of heat pump-based supply systems as they can gain heat from both solar energy and ambient air thus achieving high yields at low temperatures. The characterisation of such façades requires the modelling of the thermal performance in dependence of the wind speed. The wind speed in front of the façade is influenced by various factors such as the surroundings, the microclimate, thermal effects as well as the size of the façade. In order to model the wind dependency more accurately than in standard tests for solar thermal collectors, we carried out detailed wind field measurements on a 26 m² large active metal façade. The measurements showed that the flow behaviour in front of the façade is strongly affected by the wind direction. For wind directions parallel to the façade, we observed an almost linear velocity gradient in the vertical direction, while for wind directions perpendicular to the façade we reported a homogeneous distribution. The comparison of the measurements to wind data recorded by a nearby weather station suggests a scaling factor of 0.3 to 0.6. Based on our experimental results we performed an adjusted efficiency measurement of the metal façade and compared the yearly energy output calculated with both parameter sets. The difference is remarkable in low temperature ranges relevant for heat pump applications (i.e. 7.5% at 0°C) but negligible for operation temperatures above 10°C.

Keywords: solar thermal façades, building envelope, solar collector measurement, WISC, multi-story residential buildings, building integrated solar thermal

1. Introduction

In order to achieve net zero greenhouse gas emissions in the building sector, a significant increase of carbon-neutral heat generation technologies is required in both new and existing buildings. For this purpose, the energetic use of the building envelope is a meaningful measure, particularly for multi-story residential buildings due to their large ratio of available façade to roof area. Here, building integrated solar thermal systems can offer promising solutions with a high architectural quality (Maurer et al., 2017; Munari-Probst and Roecker, 2007). The combined use of solar thermal activated façades and heat pumps offers synergy effects such as the additional supply of environmental heat by the façades due to the low temperatures in the heat pumps evaporator (Frick et al., 2021). In particular, uncovered systems benefit from the better thermal coupling to the ambient air. Furthermore, the combination with geothermal heat pumps enables a regeneration of the ground source via the activated façades, which allows a more sustainable operation and a size-reduction of the required borehole heat exchanger field (Weiland et al., 2022; Hadorn, 2015).

Activated façades designed as uncovered solar collectors show a high dependency of the thermal performance on the wind speed due to the lack of a transparent glazing. The knowledge of this dependency is necessary to carry out performance and yield calculations and to properly dimension the heat supply system. For instance, the influence of the wind speed on the heat losses is characterized during collector performance measurements according to DIN EN ISO 9806 (2017) by determining the collector coefficients a_3 and a_6. During the measurements the wind speed is measured at one or more positions, usually outside of the collector surface area. The measured wind speed, however, can only reflect the actual wind flow velocities over the collector surface to a limited extent. Especially under natural weather conditions and with large collector arrays, the

© 2023. The Authors. Published by International Solar Energy Society
Selection and/or peer review under responsibility of Scientific Committee
10.18086/swc.2023.06.06 Available at http://proceedings.ises.org

wind field is usually highly inhomogeneous and is influenced by the surroundings, the collector surface itself and the microclimate (Simon et al., 2020). By using wind generators for the performance measurements, the resulting wind field shows different flow characteristics than the natural wind, which impacts the heat transfer between the collector surface and the ambient air. Furthermore, with large vertical facades at temperatures much higher than air temperature, the flow velocity field is overlapped by the upwards flow caused by natural convection, which is most noticeable at low wind speeds. Therefore, for large façades an estimation of the real mean wind speed over the façade and a proper positioning of the wind sensors are necessary to correctly assess its performance.

For the calculation of annual yields, location-based weather data is generally used. The wind speed is usually measured in undisturbed areas at a height of approximately 10 m (Burch and Casey, 2009). For a realistic estimation of the collector performance, the reduction of the wind speed at the collector level should be considered. For roof-installed solar thermal systems various approaches for the adjustment of the meteorological wind speed already exist: Haller et. al (2013) suggest a scaling factor of 0.5, while Burch and Casey (2009) suggest factors from 0.3 to 1, depending of the site and the height of the building. Other approaches for the calculation of wind speeds in different heights and depending on the site are the use of a logarithmic velocity profile in the atmospheric boundary layer as explained by Troen and Petersen (1990) as well as Hau (2017).

In order to obtain information about the actual wind flow velocities in front of large solar thermally active façades, we carried out wind field measurements on a test façade. After a description of the experimental setup, the paper presents and discuss the results. Furthermore, we analyzed the correlations between the wind velocities, which were measured at different positions inside and outside of the collector area, and compared them to the measurements from a nearby weather station. At last, we evaluated the performance measurement and correspondent yield calculations for the façade with the adjusted wind speed and compared them to the results based on standard procedures.

2. Experimental setup

The wind field measurements were carried out on a solar thermally active metal façade on a test stand at the Institute for Solar Energy Research in Hamelin, Germany. The test stand consists of a south-facing free-standing concrete wall with a size of 10 x 6 m² (width x height) and enables the parallel operation of two thermally active façades, each with an approximate area of 25 m². The façades are connected to hydraulic modules that allow the control of the mass flow and the inlet temperature of both façades. Moreover, the rear-side of the concrete wall is equipped with an electrical surface heating to emulate a constant interior wall temperature of a building. This measure enables the analysis of the impact of the activation on the heat flux through the wall under realistic conditions.

The test stand features an extensive measurement equipment to record the meteorological data and quantities of the façade prototypes. The meteorological station consists of two pyranometers for the measurement of the hemispherical solar irradiance in the façade plane and the horizontal plane, a pyranometer with a shadow ring for the diffuse irradiance, a pyrgeometer for the long-wave-irradiance and various sensors for measuring the ambient temperature and humidity.

To record the wind speed, three ultrasonic anemometers (MESA Systemtechnik) were installed at different positions parallel to the façade surface, which track the vertical and horizontal components of the airflow velocity in the plane in front of the façade. These were placed outside of the thermally activated area with a distance between the façade surface and the sensor of approximately 12 cm.

To characterize the façade, we used PT100-temperature immersion sensors to record the inlet and outlet temperature, PT100 surface temperature sensors for measuring the façade absorber temperatures, Coriolis flow sensors for determining the mass flow and heat flux panels to detect the heat flow through the wall structure. The façade as well as the test stand are described in more detail in (Frick et al., 2022).

Two different large-scale solar thermal activated façades were installed on the test wall: A double glazed glass façade with an active area of 22 m² and an uncovered metal façade with an active area of 26 m². Both façades feature a standard rear-ventilated design with a mineral wool insulation of 180 mm (thermal conductivity of

0.035 W m-1 K-1, ROCKWOOL Fixrock 035 VS) and a ventilation gap of 60 mm (metal façade) and 45 mm (insulation glass façade). The solar thermal activation was achieved by the application of heat exchangers on the rear-side of the claddings in the ventilation gap. In case of the metal façade, the heat exchangers were fixed with clamping profiles and threaded bolts (Frick et al., 2021). In case of the glass façade an adhesive layer was used for the connection. Fig. 1 shows the façade test stand with the installed thermally activated façades as well as the measured meteorological quantities.

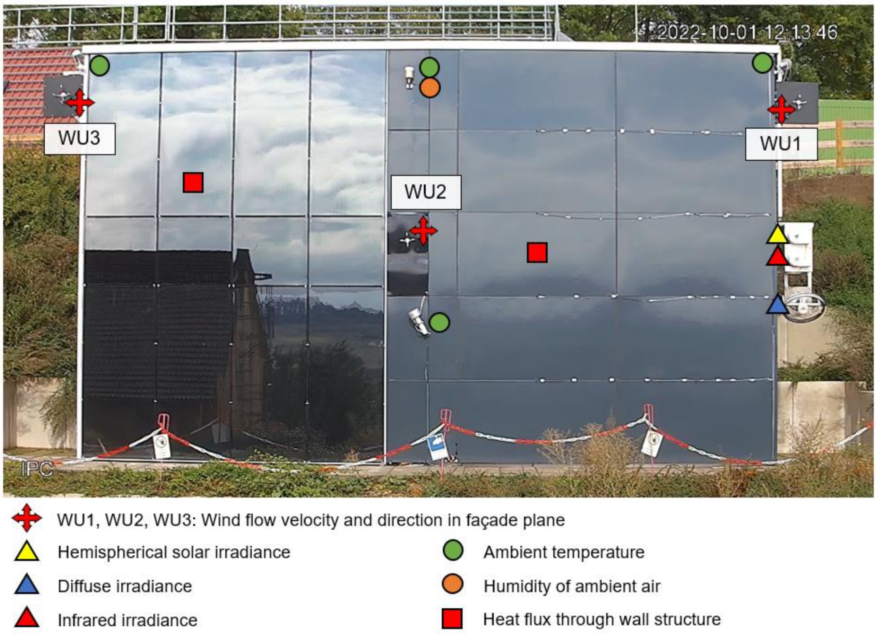

Fig. 1: Façade test stand. Left: Solar thermal active glass façade. Right: Solar thermal active metal façade.

For the wind field measurements, nine thermal anemometers (SCHMIDT Technology) were installed over the area of the activated metal façade additionally to the ultrasonic anemometers. The sensors were aligned perpendicular to the façade surface, in order to measure the absolute value of the wind flow velocity in the façade plane. Eight thermal anemometers were distributed evenly within the activated area of the metal façade, while another one was installed as a reference directly next to the central ultrasonic anemometer. In order to record the velocity of the free wind flow in front of the façade without impact of viscous effects near the façade surface, the thermal anemometers were placed at a distance of 6 cm from the façade surface, outside of the boundary layer (estimation of the maximum boundary layer thickness for the façade test stand at a wind speed of 0.1 m/s and an ambient temperature of 30°C: $\delta \approx 4.35$ cm). Fig. 2 shows the exact positions of the anemometers installed on the metal façade as well as the labeling of the individual measuring points used in this article.

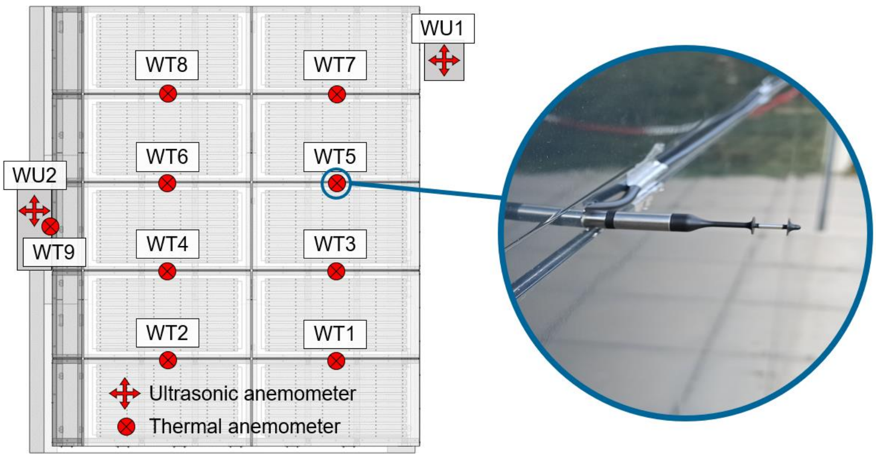

Fig. 2: Left: Positions and labels of the ultrasonic anemometers and thermal anemometers installed on the solar thermally activated metal façade. Right: Thermal anemometer installed on the metal façade with a distance of approximately 6 cm between the façade surface and the measuring probe.

The measured wind speeds are also compared to the data from a nearby freestanding weather station. The weather station is located at a distance of approximately 70 m from the façade and uses an ultrasonic anemometer to record the wind speed as well as the wind direction at a height of about 3 m above the top of the test façade.

3. Evaluation of the wind field measurements

To investigate the correlation between the flow velocities at the individual sensor positions, we carried out a sequence of measurements. To measure the flow velocities caused by the natural wind and to minimize the effects of natural convection due to temperature differences between the façade surface and the ambient air, the fluid temperature inside both test façades was controlled, so that the surface temperature of the façades approached the ambient temperature. A total of approximately 158 hours of data from 18 different days were used for the evaluation of the measurement sequence. The average wind speeds that occurred during these measurements in front of the metal façade range from 0 to 3.5 m/s. The data was recorded with a time step interval of 1 s. For the visualization of the results in the following section, these data points were averaged over 1-minute intervals.

In a first step, we compared the results of the ultrasonic anemometer WU2 to the results of the thermal reference anemometer WT9. This was done to eliminate a systematic measurement error caused by the different measurement methods used for these studies. Additionally, the distance of the thermal reference anemometer to the façade surface was varied between 6 cm and 12 cm in order to analyze the influence of the distance on the measurement results. Fig. 3 shows the comparison between the measured wind speeds of both sensors during the measurement sequence. The flow velocities measured by the thermal anemometer are plotted as data points over the simultaneously measured flow velocities of the ultrasonic anemometer:

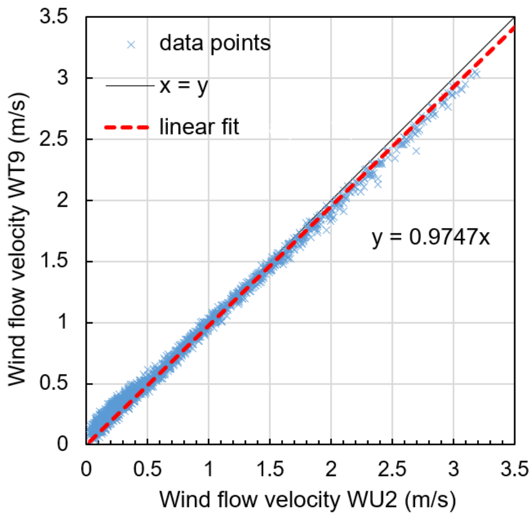

Fig. 3: Comparison between wind flow velocities measured at the ultrasonic anemometer WU2 (x-axis) and the thermal reference anemometer WT9 (y-axis). Measurement points averaged over 1-minute intervals in blue and linear regression of data points in red.

The linear regression of the data points indicates a high correlation between the results of the thermal anemometers and the ultrasonic anemometers of f(x) = 0.975x, with a relative error of approximately -2.5%. The error lies within the manufacturer's information on the measurement accuracy of both sensors, which is given as ± (5% + 0.004 m s^{-1}) for the thermal anemometer and ± 0.1 m s^{-1} for the ultrasonic anemometer. Furthermore, the variation of the thermal anemometer distance from the façade surface shows no noticeable effect on the measurement compared to the ultrasonic anemometer. Therefore, the comparison of measurements from both anemometer types provides valid results.

In a next step, the correlation between wind direction and wind speed measurement on the façade test stand was analyzed. Fig. 4 shows the distribution of wind speeds and wind directions recorded at the weather station during the wind field measurements. The diagram illustrates two dominant wind directions: west direction with wind speeds up to 10 m s^{-1} and south-southeast direction with wind speeds up to 8 m s^{-1}. On the other hand, northwest to east directions only occurred with relatively low wind speeds below 2 m s^{-1}. Similar results were reported during other experiments at ISFH by Lampe et al. (2019). Because of the south orientation of the façade test stand, the majority of the airflow toward the test façades is either parallel to the façade plane (with wind direction west) or perpendicular to the façade plane (with wind direction south).

To analyze the impact of the wind direction on the wind speed measurement in front of the façade, two different data sets filtered by the wind direction are considered separately in the following section (compare Fig. 4a: green - wind direction south-southeast from 95° to 220°, red - wind direction west from 230° to 310°). Fig. 4 b) to d) depict the vertical and horizontal component of the measured wind speed in the façade plane by the ultrasonic anemometers WU1, WU2 and WU3. A data point in the upper left quadrant thus represents an upward flow in the eastern direction. For west direction, the diagrams show a similar distribution of the data points for all three sensors: As expected the measured airflow near the façade surface is mostly towards the eastern direction and airflow in other directions only occurs with low flow velocities. Here, the anemometer WU3 records slightly higher maximum velocities than the other two with up to 3.5 m s^{-1} (WU1: approximately 3 m s^{-1}, WU2: approximately 2 m s^{-1}). This indicates a slight velocity gradient in the vertical direction with wind direction parallel to the façade surface. Furthermore, the sensor WU1 mainly records airflow with an upward component, while the other two sensors also record downward airflow.

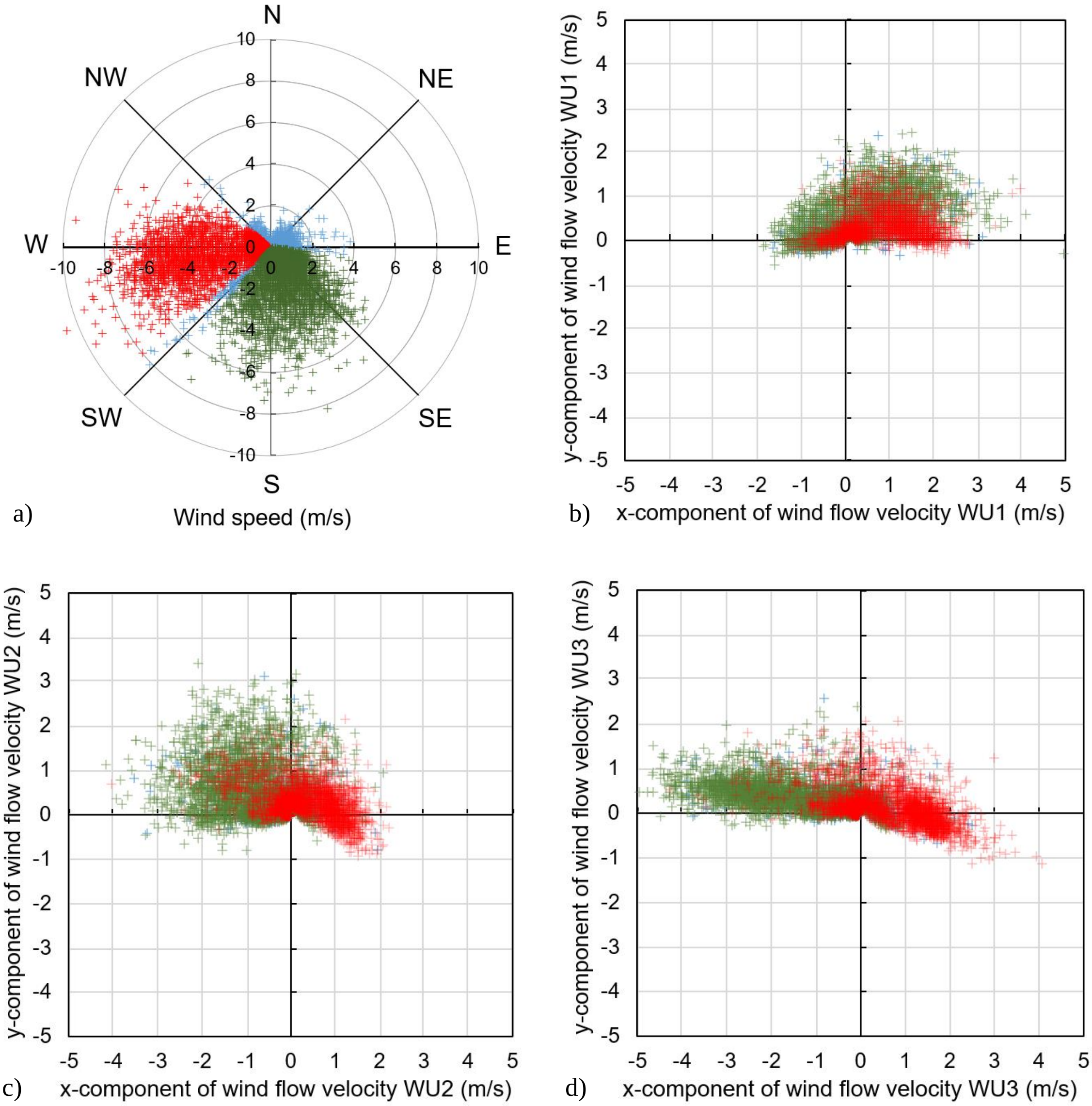

Fig. 4: a) Distribution of measured wind speeds and wind direction at the ISFH weather station during the wind field measurements. b) to d) Vertical (y-axis) and horizontal (x-axis) components of the measured wind flow velocity in the façade plane on the ultrasonic anemometers WU1, WU2, WU3. Red: Data points for west direction (230° to 310°). Green: Data points for south-southeast direction (95° to 220°). Blue: Remaining data points.

For wind direction south-southeast, the distribution of the recorded data points differs significantly from each other: While the anemometer WU1 mainly detects airflow to the eastern direction as in the previous example, WU2 and WU3 show a high tendency for airflow to the western direction. Furthermore, the sensor WU3 also records significantly higher velocities than WU1 and WU2 with up to approximately 4.5 m s^{-1} (WU1 and WU2 both show a maximum of about 3 m s^{-1}, although in different directions). The different behaviour of the airflow at the three positions can be explained by the specific installation of the sensor WU3, which is unobstructed towards the western direction. Wind that comes from southeast can flow in this direction mostly undisturbed, while at sensor WU1 the airflow to the west is restricted by the surface of the façade and thus tends to flow in the eastern direction. For the central sensor WU2 the wind is in this case obstructed in both directions so that airflow with a significant upwards component occurs. Therefore, with wind directions perpendicular to the façade surface, the positioning of the anemometers has a significant effect on the measurement results.

In the next step, the deviation of the flow velocity at the different sensor positions to the mean wind speed in front of the façade was investigated. For this purpose, the mean wind speed was defined as the average value of the measured flow velocities from the thermal anemometers WT1 to WT8, which were distributed evenly over the façade area. Fig. 5 shows an example of the measured data points in the upper (mean value form WT7 and WT8) and in the lower (mean value from WT1 and WT2) area of the façade plotted over the defined mean wind speed over the façade. The mean value was calculated because sensors at the same installed height show a similar behaviour. Again, two different data sets filtered by the wind direction west (red) and south-southeast (green) were considered for the analysis. For a better visualization the data points were averaged over 5-minute intervals.

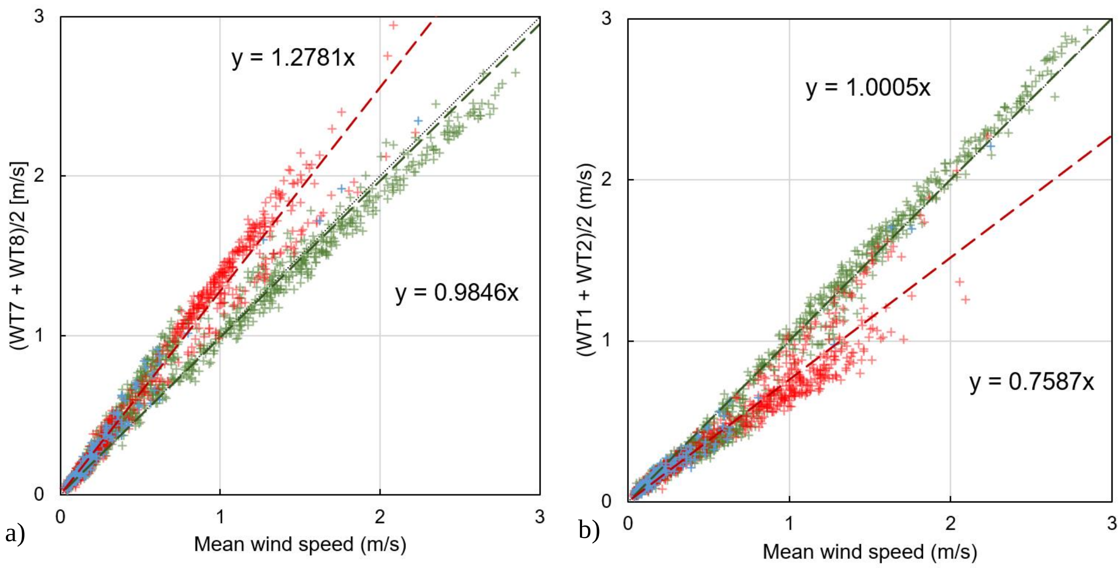

Fig. 5: Correlation between measured wind flow velocities in the upper (a) and lower (b) area of the activated metal façade and the mean wind speed over the façade. Measured data points averaged over 5-minute intervals. Red: West direction. Green: South-southeast direction. Blue Remaining data points.

The diagrams show that the trend of the data points is highly dependent on the considered wind direction. For south-southeast direction, the linear regression of the data points is nearly 1.0. Therefore, the measured flow velocities correspond precisely to the mean wind speed over the façade. In this case, the correlation indicates that there is a homogeneous wind field in front of the façade with only small deviations from the mean wind speed. For west direction, the regression for the flow velocity is approximately 1.28 in the upper façade area and 0.76 in the lower façade area. For a mean wind speed of 1.5 m s^{-1} the difference in the flow velocity between the lower and upper area is therefore about 0.78 m s-1. Tab. 1 lists the scaling factors for the mean wind speed for all installed anemometers on the façade test stand as well as the nearby weather station for the considered wind directions. Furthermore, Fig. 6 shows the scaling factors as a function of the installation height of the respective anemometer on the test façade.

Tab. 1: Scaling factors to the mean wind speed over the façade for the installed anemometers for wind directions west and south-southeast

	WT1	WT2	WT3	WT4	WT5	WT6	WT7	WT8
west	0.74	0.78	0.96	0.91	1.02	1.04	1.28	1.28
south-southeast	0.99	1.00	1.07	1.06	0.93	0.97	0.99	0.97
	(WT1 + WT2)/2		**(WT3 + WT4)/2**		**(WT5 + WT6)/2**		**(WT7 + WT8)/2**	
west	0.76		0.93		1.03		1.28	
south-southeast	1.00		1.06		0.95		0.98	
	WU1		**WU2**		**WU3**		**Weather station**	
west	1.29		1.05		1.33		3.49	
south-southeast	0.96		1.10		1.45		1.71	

The scaling factors of the remaining anemometers and the plot as a function of the installation height confirm the previous statements: In case of wind direction perpendicular to the façade, both the thermal anemometers and the ultrasonic anemometers WU1 and WU2 show scaling factors near 1.0. Therefore, the wind field over the metal façade is homogeneous. The ultrasonic anemometer WU3, that is installed on the glass façade, records considerably higher flow velocities with a scaling factor of around 1.45 due to the unobstructed positioning in the western direction, for the already mentioned reasons. The comparison of the data from the weather station shows that measured wind speeds are approximately 1.71 times higher than in front of the façade.

For wind direction parallel to the façade, the results show a strong correlation between the scaling factors and the installation height of the anemometer on the façade with an almost linear behaviour. The scaling factor increases by approximately 0.142 per meter. Accordingly, at a mean wind speed of around 1.5 m s^{-1} the wind field shows a flow velocity gradient of approximately 0.213 m s^{-1} per meter in the vertical direction. The scaling factors of the ultrasonic anemometers also confirm this behaviour regardless of their positioning relative to the façade test stand. Thus, WU1 and WU3 have similar scaling factors at the same installation height. The weather station records approximately 3.49 times higher velocities compared to the mean wind speed in front of the façade.

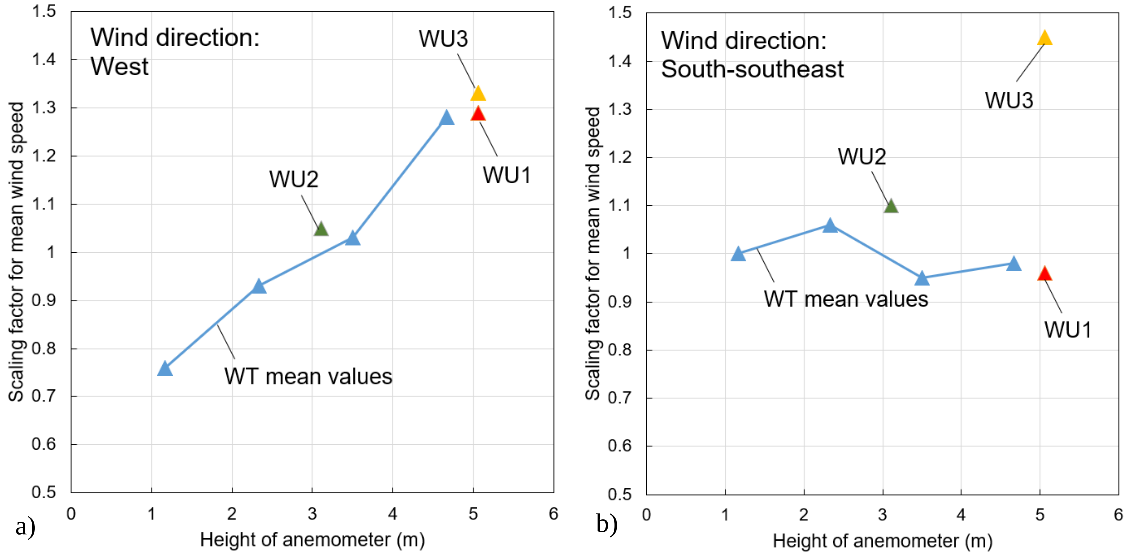

Fig. 6: Dependence of the scaling factor of the installed anemometers to the mean wind speed from the installation height on the test façade. a) Wind direction west. b) Wind direction south-southeast.

4. Performance measurements with adapted wind speed

The results of the wind field measurement were included in the performance measurement of the façade in order to model the influence of the wind speed on the collector performance of the façade more accurately. In the following section, the comparison of the performance characterization with and without adaptation of the reference wind speed is presented.

Frick et al. (2022) demonstrated the performance characterization of the large-scale active metal façade using the quasi-dynamic testing procedure (QDT) as well as a comparison to the steady-state performance measurement (SST) of a single module of the metal façade in the ISFH sun-simulator. It should be noted that the characterization was carried out without the reduction of the wind speed by a constant 3 m s^{-1} according to the DIN EN ISO 9806 (2017), because wind speeds above 3 m s^{-1} rarely occur in front of the façade. A valid evaluation of the parameters a_3 and a_6 is therefore only reasonable without this adjustment. Tab. 2 summarizes the determined collector parameters and compares it to adjusted values that have been calculated by using the adapted wind speed from this study.

Tab. 2: Results of the performance characterization of the solar thermally active metal façade. Indoor steady-state measurement (SST) on a single module as well as outdoor quasi-dynamic measurement (QDT) on the large-scale façade with and without adjustment of the reference wind speed.

Parameter	**ṁ** kg/hm²	**$\eta_{0,hem}$ / $\eta_{0,b}$**	**K_d** -	**r** -	**a_1** W/m²K	**a_3** J/m³K	**a_4** -	**a_5** J/m²K]	**a_6** s/m
SST-Indoor Single module	60	0.56	-	-	9.86	**1.22**	0.58	-	**0.0386**
QDT-Outdoor Without adapted wind	60	0.59	0.98	0.159	11.33	**0.103**	0.212	22755	**0.0144**
QDT-Outdoor With adapted wind	30	0.55	0.98	0.159	10.96	**1.10**	0.212	22755	**0.0097**

It can be seen that the wind-dependency of the heat loss coefficient a_3 is significantly lower for the outdoor measurement with 0.103 J m^{-3} K^{-1} than for the laboratory measurement with 1.22 J m^{-3} K^{-1}. The comparison to the parameters of common uncovered collectors also shows, that a much higher value for a_3 should be expected than that determined with the outdoor tests. The low a_3 value can be explained by two reasons: First of all, the ultrasonic anemometer WU1 was used for the reference wind speed to evaluate the collector coefficients. As shown in the previous section of the article, during wind direction west, WU1 records flow velocities that are approximately 29% higher than the mean wind speed on the façade.

The effect of the wind speed on the heat losses is thus underestimated in the evaluation. Secondly, the used reference anemometer is located directly next to the investigated façade. This means that with higher façade temperatures the anemometer measures airflow due to the natural convection additionally to the natural wind airflow. The measured velocities at higher absorber temperatures are thus always larger than at low absorber temperatures, which again leads to an underestimation of the effect of the wind speed on the heat losses at higher temperature points. This effect becomes more significant during test periods with generally low wind speeds.

For the adjusted values, the ultrasonic anemometer WU3, that is located near the glass façade, was chosen as the reference wind sensor for the evaluation. During the performance measurements, the temperature of the glass façade was controlled to approach the ambient temperature, to minimize the effect of natural convection on the sensor WU3. During the performance measurements, both wind directions south and west were recorded at the weather station. As shown in section 3, WU3 detects velocities approximately 33% above the mean wind speed in front of the metal façade for wind direction west and 45% higher velocities for wind direction south (Tab. 1). To adjust the measured value at position WU3 to the mean wind speed of the metal façade, the data was scaled by a factor of 0.72 (mean value of 1/.133 and 1/1.45). Wind speeds with a maximum of approximately 3 m s^{-1} were recorded on the metal façade during the adapted performance measurements. For the quasi-dynamic evaluation of the collector coefficients, the recorded data was averaged over 30-second intervals. The incident angle modifiers for direct and diffuse radiation as well as the collector parameters a_4 and a_5, which were determined during the first performance measurement, were not evaluated again to avoid correlations between the coefficients and to be able to focus on the effect on the parameters a_1, a_3 and a_6.

The results show, that the zero-loss efficiency with 0.55 is slightly smaller for the adjusted performance measurements than for the regular performance tests with 0.59. The reason for this deviation is the different fluid mass flow set during the measurements. The regular measurement was carried out with a specific mass flow of 60 kg h^{-1} m^{-2}, which ensures a turbulent flow inside of the heat exchangers over the full temperature range. For the adjusted performance measurement, which was carried out during long-term tests under typical operation conditions, the specific mass flow was set to 30 kg h^{-1} m^{-2}, which leads to a laminar flow and a less efficient heat transfer in the heat exchangers at lower fluid temperatures.

The heat loss coefficient a_3 from the adjusted performance measurement is much closer to the results from the laboratory test and the expected value for an uncovered collector. With the adjusted measurements the correlation between the wind speed and the collector performance is thus estimated more accurately.

To visualize the effect of the higher a_3 value, we calculate the expected thermal output of the façade using the standard collector model from DIN EN ISO 9806 (2017) with the coefficients from Tab. 2. The zero-loss efficiency of the adapted coefficients was set to 0.59 to compensate for the different fluid mass flow during measurements. Fig. 7 a) shows a comparison between the modelled thermal output for the characterization with and without adjusted wind speed measurement at a solar irradiation of G_{Hem} = 1000 W m^{-2} for three different wind speeds.

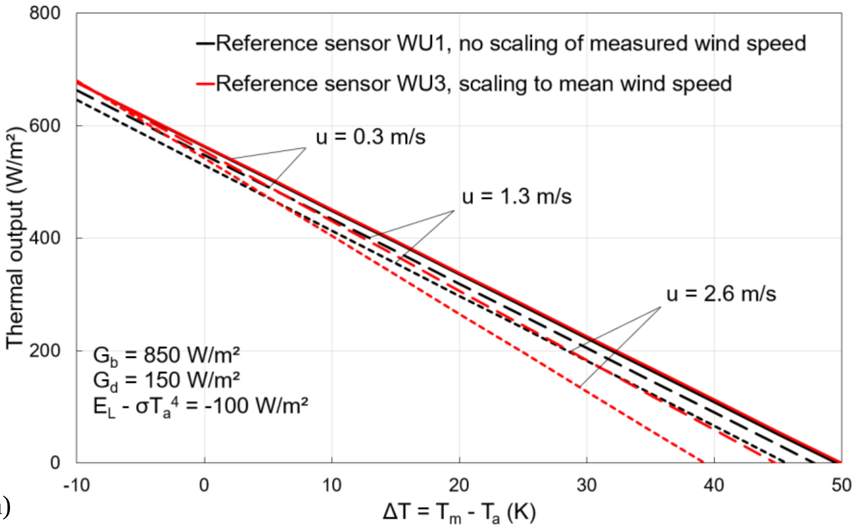

a)

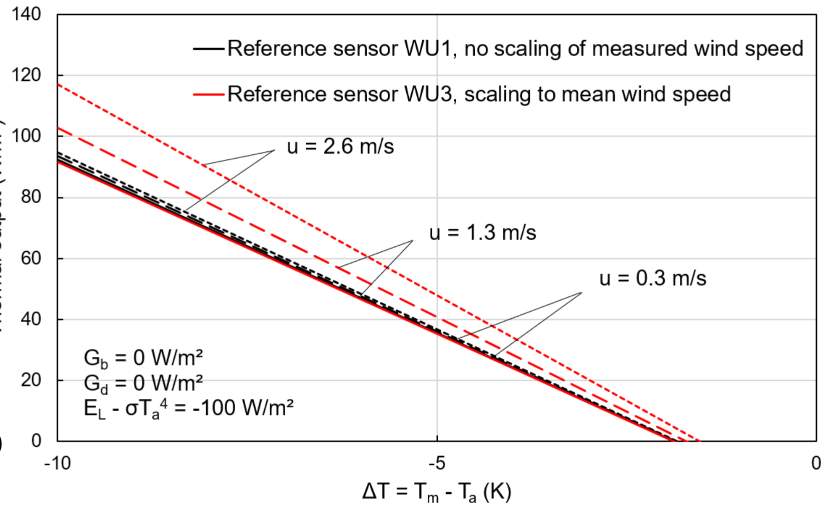

b)

Fig. 7: Comparison of the efficiency curves of the solar thermal active metal façade for performance characterization with and without adjusted wind speed measurement. a) Efficiency curves for solar irradiation G_{Hem} = 1000 W m^{-2}. b) Without solar irradiation.

The diagrams show that, without adjustment of the wind measurement, the wind speed has no significant effect on the collector efficiency apart from a slight parallel shift of the performance curves. Due to the higher a_3 value from the adjusted performance tests, the efficiency curves for different wind speeds diverge significantly with higher temperature differences. Furthermore, the maximum temperatures, at which the metal façade is able to generate heat, differ for both performance characterizations: Without the adjustment, the stagnation temperature drops by approximately 3 K at a wind speed of 2.6 m s^{-1} compared to 0.3 m s^{-1} (49 K to 46 K), while it drops by about 10 K with the adjusted measurement (47 K to 37 K). Fig. 7 b) shows the thermal output for the façade as an environmental heat exchanger without solar irradiation. The comparison shows that the effect of the more accurate a_3 value increases significantly with higher temperature differences.

The different behaviour of the thermal output has an impact on the results of annual yield simulations. To estimate the effect, gross thermal yield calculations were carried out for the active metal façade with the calculation tool ScenoCalc (ESTIF) using both sets of collector coefficients. Fig. 8 shows the results of the yield calculations for a south oriented façade with weather data from Würzburg, Germany as a function of the mean fluid temperature inside the façade. The meteorological wind speeds were scaled with a factor of 0.5 for the calculations. As for the performance measurements, the wind speeds were not reduced by a constant 3 m s^{-1} according to DIN EN ISO 9806 (2017).

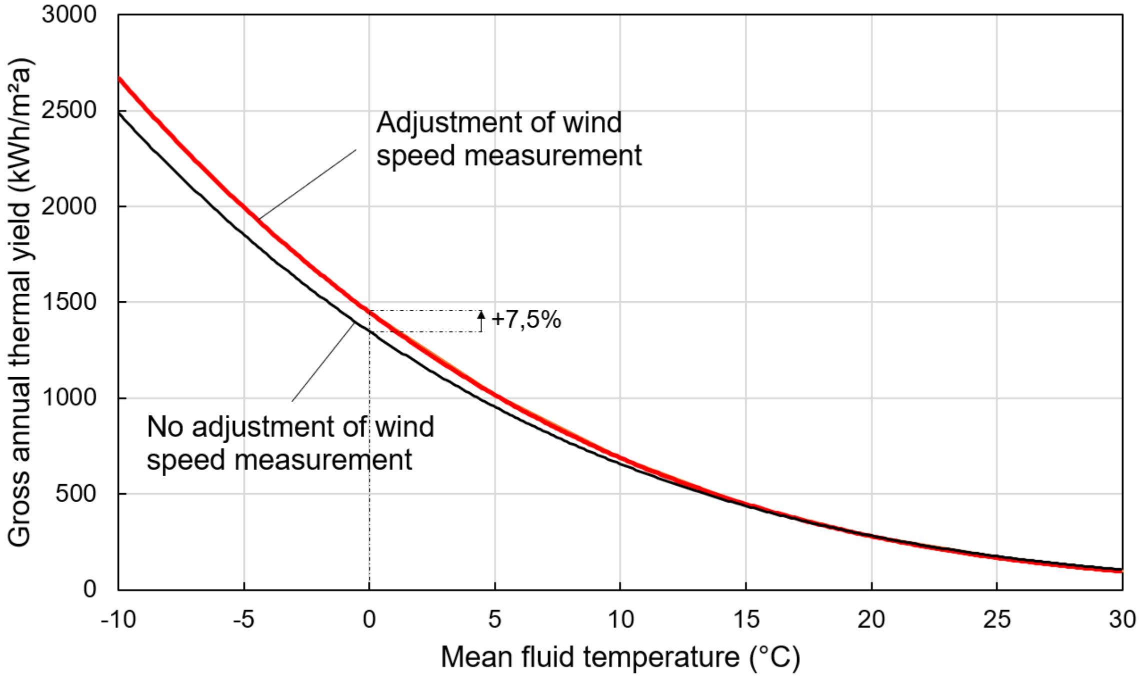

Fig. 8: Comparison of the gross annual thermal yield for the solar thermal active metal façade using the collector coefficients with and without adjusted wind speed measurement. Calculation of the gross thermal yield with ScenoCalc (ESTIF) for a south oriented façade with weather data from Würzburg, Germany.

The diagram illustrates that the main effect of the wind-dependency is noticeable at low temperatures, because the façade mainly operates as an environmental heat exchanger in that temperature range. At a mean fluid temperature of 0°C (e.g. for an application of the façade as a heat pump source or for the regeneration of ice storages) the calculated gross annual thermal yield is approximately 101 kWh m^{-2} a^{-1} higher (relative deviation of 7.5%) when using the coefficients for the accurate wind dependency. At higher temperature both yield curves converge. The effect of the wind speed becomes smaller because the façade operates mainly as a solar absorber and less as an environmental heat exchanger. For applications in temperature ranges above 10°C the relative deviation is below 5% and thus, the impact of the real wind speed is negligible if compared to the results based on performance measurements according to standard procedures.

5. Summary

The paper presents investigations on the effect of the wind speed on the thermal behaviour of solar thermal active façades, which are designed as uncovered collectors. For the investigations, we carried out a wind field measurement on a rear-ventilated metal façade at our façade test stand. For this purpose, a set of thermal anemometers were installed on the test façade in addition to the three already installed ultrasonic anemometers: Eight of the thermal anemometers were distributed evenly within the active area of the metal façade. At the same time, wind data from a nearby weather station was used for the evaluation.

The evaluation of the wind field measurement showed that the two dominant wind directions have a significant influence on the behaviour of the airflow on the façade. With an airflow parallel to the façade surface, a distinctive flow velocity gradient in the vertical direction could be observed. The deviation from the mean wind speed in front of the façade can be approximated as a linear function of the vertical position. The scaling factor for the mean wind speed increases by approximately 0.142 per meter. Also, for this case the positioning of the anemometers inside or outside of the façade area seems to be negligible. For perpendicular airflow on the façade surface the measurements showed that a highly homogeneous wind field in front of the façade is. All the thermal anemometers installed inside the façade area showed similar results. When placing wind sensors outside of the façade area, however, the positioning can affect the measurement results. The comparison to the measured data from the nearby weather station indicate scaling factors of 1.71 to 3.49 depending on the wind direction. These results confirm the adjustment factors of the meteorological wind speeds proposed by Haller et al. (2013) as well as Burch and Casey (2009).

An adjusted performance characterization of the solar thermal active metal façade was carried out with the results from the wind field measurements. The characterization showed that by minimizing the effect of the natural convention of the façade on the reference anemometer and adjusting the measured wind speeds with scaling factors from the wind field measurement, an accurate model for the wind-dependency of the heat losses can be obtained, which is significantly closer to the expected values of uncovered solar collectors and to the values from the laboratory measurements on a single façade module.

The effect of the accurate representation of the wind dependency is most noticeable in yield simulations with generally low fluid temperatures. A comparison of the gross annual thermal yields of the active metal façade shows that with a more accurate model for the wind dependency a 7.5% higher yield is predicted at fluid temperatures around 0°C. This is particularly significant for low-temperature applications such as the regeneration of ice storages or the use of the façade a as heat source for heat pumps.

It should be noted that the results of this work refer to the specific configuration of the façade test stand at the ISFH and are influenced by the surroundings and the microclimate. In order to verify the general applicability of the results to other configurations, a comparison of the results to measurements from other façades and at various locations is necessary.

6. Acknowledgments

The work is based on the results of the project "Solar-VHF", funded by the Lower Saxony Ministry of Science and Culture and by the German Federal Ministry of Economic Affairs and Climate Action (BMWK, reference number 03ETW013A), following a decision of the German Parliament. The investigations are carried out in cooperation with the Fraunhofer-Institut für Bauphysik IBP and the German companies Konvortec GmbH & Co. KG, Systea Pohl GmbH, Gundlach GmbH & Co. KG Wohnungsunternehmen, Pforzheimer Bau und Grund GmbH and Clina Heiz- und Kühlelemente GmbH. The authors are grateful for the support and responsible for the content of the publication.

7. References

Burch J., Casey R., 2009. Wind issues in solar thermal performance ratings. National Renewable Energy Laboratory, Buffalo, New York. Available at https://www.osti.gov/servlets/purl/952890 (Accessed 10 October 2023)

DIN EN 9806:2018-04, 2018. Solar energy – Solar thermal collectors – Test methods (ISO 9806:2017); German version EN ISO 9806:2017. Beuth Verlag GmbH. https://dx.doi.org/10.31030/2681379

ESTIF, 2019. ScenoCalc tool (Solar Collector Energy Output. European Solar Thermal Industry Federation (ESTIF).

Frick E., Büttner C., Kirchner M., Giovannetti F., 2021. Solar thermal, rear-ventilated façades as heat pump sources in multi-storey buildings. *ISES Solar World Congress*, Online Conference, 25-29 October.

Frick E., Kirchner M., Büttner C., Wehmeier T., Giovannetti F., 2022. Dynamische Charakterisierung solarthermisch aktiver Fassaden als Quelle für Wärmepumpensysteme. *32. Symposium Solarthermie und innovative Wärmesysteme*, Bad Staffelstein, 3-5 May.

Hadorn J.-C., 2015. Solar and Heat Pump Systems for Residential Buildings. Ernst & Sohn, Hoboken.

Haller M. Y., Dott R., Ruschenburg J., Ochs F., Bony J., 2013. The Reference Framework for System Simulations of the IEA SHC Task 44 / HPP Annex 38 Part A: General Simulation Boundary Conditions A technical report of subtask C Report C1 Part A. IEA Solar Heating and Cooling Programme. http://dx.doi.org/10.13140/2.1.2221.4727

Hau E., 2017. Windkraftanlagen: Grundlagen. Technik. Einsatz. Wirtschaftlichkeit, 6. Aufl. Springer Berlin Heidelberg, Berlin, Heidelberg.

Lampe C., Kirchner M., Littwin M., Giovannetti F., Asenbeck S., Fischer S., 2019. Experimentelle Untersuchungen an Testfeldern mit SOLINK-photovoltaisch-thermischen Kollektoren. *29. Symposium Solarthermie und innovative Wärmesysteme*, Bad Staffelstein, 21-23 May.

Maurer C., Cappel C., Kuhn T. E., 2017. Progress in building-integrated solar thermal systems. Solar Energy 154, 158-186. https://doi.org/10.1016/j.solener.2017.05.065

MESA Systemtechnik GmbH, 2023. MESA WSWD SONIC Anemometer Datenblatt [Online]. Available at https://mesa-systemtechnik.de/datenblaetter/WSWD_Sonic.pdf (Accessed 10 October 2023)

Munari-Probst M. C., Roecker C., 2007. Towards an improved architectural quality of building integrated solar thermal systems (BIST). Solar Energy 81, 1104-1116. https://doi.org/10.1016/j.solener.2007.02.009

ROCKWOOL GmbH Co. KG, 2023. Fassadendämmplatte Fixrock 035 VS Datenblatt [Online]. Available at https://p-cdn.rockwool.com/syssiteassets/rw-d/datenblatter/fassade-vhf/db-fixrock-035-vs-rockwool.pdf?f=20220801092500 (Accessed 10 October 2023)

SCHMIDT Technology GmbH, 2023. SCHMIDT Strömungssensor SS 20.250 Datenblatt [Online]. Available at https://www.schmidttechnology.de/wp-content/uploads/wpallimport/files/api_files/downloads/SS_20.250_de.pdf (Accessed 10 October 2023)

Simon, H., Bruse M., Cramer L., Sinsel T., 2020. Improving Building Performance Simulation boundary conditions. *PLEA: Passive and Low Energy Architecture*, Coruna, 1-3 September.

Troen I., Lundtang Petersen E., 1989. European Wind Atlas. Risø National Laboratory, Roskilde.

Weiland F., Kracht N., Chhugani B., Pärisch P., 2022. Techno-Economical Assessment of a Solar Regenerated Borehole Heat Exchanger Field with PVT Collectors for District Heating. *EuroSun*, Kassel, 25-29 September.